Millimeter Wave Picocellular System Evaluation for Urban Deployments

Mustafa Riza Akdeniz, Yuanpeng Liu, Sundeep Rangan, Elza Erkip
Polytechnic Institute of New York University, Brooklyn, New York
Email: {makden01,yliu20}@students.poly.edu, {srangan,elza}@poly.edu

***Abstract*—With the severe spectrum shortage in conventional cellular bands, millimeter wave (mmW) frequencies between 30 and 300 GHz have been attracting considerable attention as a possible candidate for next-generation micro- and picocellular wireless networks. The mmW frequency bands offer orders of magnitude greater spectrum than current cellular microwave frequencies currently deployed below 3 GHz. However, even with typical microcellular radii of 100m to 200m, the propagation of mmW signals in outdoor non line-of-sight (NLOS) links remains challenging and the feasibility of such mmW networks is far from clear. This paper uses recent real-world measurements at 28 GHz to provide the first systematic assessment of mmW picocellular networks. It is found that, even with its limited propagation characteristics, mmW systems can offer an order of magnitude increase in capacity over current state-of-the-art 4G cellular networks with similar cell density. However, it is also shown that such mmW networks will operate in an extremely power-limited regime where the full spatial and bandwidth degrees of freedom are not fully utilized. This power-limited regime contrasts significantly with current bandwidth-limited cellular systems, requiring alternate technologies for mmW systems that may unlock further gains that mmW frequency bands offer.**

I. Introduction

With the popularity of today's smartphones and tablets, demand for cellular wireless data is projected to grow at a staggering rate [1]. This trend is necessitating new technologies that can offer orders of magnitude increases in network capacity. To address this challenge, there has been growing interest in cellular systems based in the so-called *millimeter-wave* (mmW) bands, between 30 and 300 GHz, where the available bandwidths are much wider than today's cellular networks [2]–[4]. The available spectrum at these frequencies can be easily 200 times greater than all cellular allocations today that are currently largely constrained to prime RF real estate under 3 GHz. Moreover, the very small wavelengths of mmW signals combined with advances in low-power CMOS RF circuits enable large numbers of miniaturized antennas to be placed in small dimensions. These multiple antenna systems can be used to form very high gain, electrically steerable arrays, fabricated at the base station, in the skin of a cellphone, or even within a chip [4], [5].

However, while mmW communication has successfully used for backhaul and short-range indoor communication [6]–[8], its applicability to longer range wide-area networks remains challenging and the feasibility of such systems remains an open question. Most importantly, the propagation of mmW signals is much less favorable than signals in conventional microwave frequencies. Due to the higher frequencies, Friis' transmission law implies an immediate increase of 20 to 30 dB in free-space path loss. Moreover, mmW signals can be extremely shadowed from many obstacles such as brick [2].

To assess the feasibility of these networks, Rappaport *et. al.* [9]–[12] performed an extensive set of measurements to characterize NLOS propagation of mmW signals in New York City at 28 GHz. To mimic microcellular type links for such areas, transmitters were placed on rooftops, two to three stories high, and path loss measurements were then made at a number of street-level locations up to 200m from the transmitters.We review the measurement methodology and resulting path loss and shadowing models in Section II.

The broad purpose of this paper is to use these measurements to provide the first systematic evaluation of mmW picocellular networks in a dense urban environment based on real experimental data. We focus on urban outdoor environments since the high user density, small cell radii (typically 100 to 200m) and lower mobility makes urban settings a natural candidate for initial deployments of mmW picocellular networks. However, at the same time, the urban topology is a particularly challenging setting for mmW signals due to the lack of LOS connectivity, severe shadowing as well limitations on the height and placement of cells.

To assess the capacity of these systems, this paper uses the models derived in [9]–[12] with an industry-standard microcellular 3GPP evaluation framework [13], [14] to estimate both the capacity and cell edge throughput under various deployment and device options.

Our key finding is that mmW picocellular networks offer a possible order of magnitude increase in capacity over current cellular systems. Specifically, our simulations show that a hypothetical 1 GHz TDD mmW picocellular network offers more than 30x capacity over a over an LTE 10+10 MHz 2x2 FDD LTE system with similar deployment assumptions and capacity estimates in [13]. Nevertheless, our simulations also indicate that mmW systems are potentially severely power-limited and thus operate in a fundamentally different regime than current cellular networks in dense interference-limited deployments. As a consequence, the enormous bandwidth and spatial degrees of freedom afforded by mmW spectrums are not fully utilized in the current cellular deployment model. As part of future research, we suggest alternate technologies

such as multihop relaying that may be able to unlock these degrees of freedom and increase the gains of mmW systems even further.

While there has been some recent work on system level evaluation of mmWave systems, [2], [15], [16], ours is the first one based on real mmWave measurements in urban environment. The paper [2] uses a free-spaced-based path loss while [15] assumes a ray tracing model, both of which tend to underestimate the channel attenuation. Furthermore, [16] does not focus on an urban scenario, and assumes LOS connections with minimal scattering, which again result in overly optimistic capacity gains. Finally, we focus on a mmW picocellular system, where random deployment is assumed as opposed to a sectorized microcellular system studied in [2].A full version of the paper with greater modeling details, simulations and discussions in available in [17].

II. Measurements and Path Loss Models

With the development of 60 GHz LAN and PAN systems, millimeter wave signals have been extensively characterized in indoor environments [18]–[23]. However, models for mmW propagation in outdoor settings suitable for estimating picocellular system capacity have only recently appeared [9], [15], [24]–[26].

The path loss and multi-input multi-output (MIMO) spatial models in this study are based on recent 28 GHz measurements in New York City [9], [11]. To characterize both the bulk path loss and spatial structure of the channels, measurements reported in [9], [11] were made with highly directional horn antennas (10 degree beamwidths, 24.5 dBi gain each side). At each transmitter (TX) - receiver (RX) location pair, the angles of the TX and RX antennas were swept across a range of values to detect discrete clusters of paths. Empirical statistical models were then fit to this data to describe a variety of channel characteristics including the number of clusters, path loss per cluster, cluster angular spread, etc.

The resulting parameters of the evaluation model assumed in this study are summarized in Table I. The parameters are based both on the original papers [9], [11], as well as extended models that will be presented in a submitted paper [12]. As described in Table I, the channel between each TX-RX pair is assumed to consist of $K = 3$ clusters, with the path loss of each cluster of the form $\alpha + 10\beta \log_{10}(d)$ with independent lognormal shadowing and α, β taken from [12]. The measurements in [11] reported minimal horizonal angular spread at the TX or vertical angular spread at either the TX and RX. Hence, the evaluation model here assumes that the BS central horizontal angle of departure (AoD) and all vertical angles are the same for all clusters. However, the angle-of-arrivals (AoA) of the $K = 3$ clusters at the UE are independent and distributed uniformly in $[0, 2\pi]$. Following [11], the subpaths within each cluster are then generated uniformly with in an interval of $[-\delta, \delta]$ around the central angle of the clusters.

For comparison, Fig. 1 plots the path loss model used in this paper along with several previous models. The model used in this paper, as described above, is shown on the curve labeled

TABLE I: Path loss and beamforming parameters

Parameter	**Value**
Number of clusters K	3
Per cluster shadowing S_k	*Lognormal* $(0, \sigma)$, $\sigma = 8.36$ dB
Per cluster path loss PL_k	$PL_k = 75.85 + 37.3 \log_{10}(d) + S_k$, d in meters
BS and UE vertical central cluster AoD and AoA, $\bar{\phi}^T$ and $\bar{\phi}^R$	Single value common to all BS and UEs and clusters within each BS and UE. No vertical angular separation is assumed.
BS horizontal central cluster AoD, $\bar{\theta}_k^T$	*Uniform*$[0, 2\pi]$, common to all clusters from the BS.
UE horizontal central cluster AoA, $\bar{\theta}_k^R$	*Uniform*$[0, 2\pi]$, independent for all clusters from the UE.
BS and UE cluster vertical angular spread	0
BS and UE cluster horizonal angular spread, $2\delta_k$	*Exponential*(λ) mod $360°$, $\lambda^{-1} = 7.8°$. Common to all clusters from BS, but independent between clusters to UE. Subpaths generated uniformly with angles $[-\delta, \delta]$ around horizontal AoA and AoD.

"empirical NYC". The curve shows the effective average *omnidirectional* path loss found by non-coherent combining of the energy across all K clusters See [17] for details. It is immediately seen that this path loss is significantly higher than several other models:

- *Free-space:* The theoretical free space path loss is given by Friis Law [27]. We see that, at $d = 100$ m (our target cell radius), the free-space path loss is more than 43 dB less than the model we have assumed here.
- *PLF1, PLF2:* These are two models used in Samsung study [2]. The first model, PLF1, is simply free space propagation plus 20 dB, while the second model, PLF2, is a theoretical extrapolation of microwave propagation models. Both models are consistently more than 20 dB lower than our model.
- *3GPP UMi:* The standard 3GPP urban micro (UMi) model with hexagonal deployments [13] is given by

$$PL(d) = 22.7 + 36.7 \log_{10}(d) + 26 \log_{10}(f_c), \quad (1)$$

where d is distance in meters and f_c is the carrier frequency in GHz. It can be seen that, relative to the 3GPP UMi model at f_c=2.5 GHz, the empirical 28 GHz model shows approximately 40 dB greater path loss.

We conclude that the mmW propagation model used here is significantly worse than path losses in current microwave frequencies as well as free space and other models used in earlier evaluation studies of mmW systems. As described above, this high path loss is a result of the NLOS propagation assumption implicit in the data on which the models are based. Nevertheless, we will see that with appropriate beamforming, mmW systems can still offer an order of magnitude improvement in capacity.

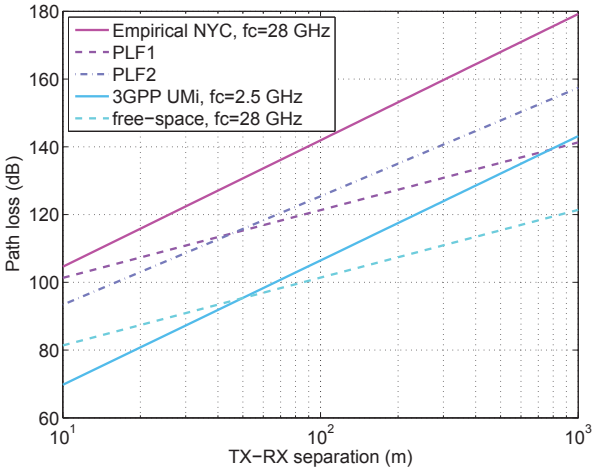

Fig. 1: Comparison of empirical path loss model based on NYC data [9], [11] against 3GPP Urban Micro path loss model [13] at $f_c = 2.5$ GHz and 28 GHz. It can be seen that the mmW frequencies result in an approximately 40 dB loss.

TABLE II: Default network parameters

Parameter	**Description**
Network layout	BS, UE uniformly dropped in a 2km x 2km square area
Average inter-site distance (ISD)	200 m
Number UEs	10 per cell
Carrier frequency	28 GHz
Duplex mode	TDD
Transmit power	20 dBm (uplink), 30 dBm (downlink)

III. System Modeling

A. Network topology

We follow a standard cellular evaluation methodology [13] where the base stations (BSs) and user equipments (UEs) are randomly "dropped" according to some statistical model and the performance metrics are then measured over a number of random realizations of the network. Since we are interested in picocellular networks, we follow a BS and UE distribution similar to the 3GPP Urban Micro (UMi) model in [13] with some parameters taken from the Samsung mmW study [2], [3]. The specific parameters are shown in Table II. Similar to 3GPP UMi model, the base station cell sites are distributed in a uniform hexagonal pattern with three cells (sectors) per site covering a 2 km by 2 km area with an inter-site distance (ISD) of 200 m. This layout leads to 130 cell sites (390 cells) per drop. UEs are uniformly distributed over the area at a density of 10 UEs per cell which also matches the 3GPP UMi assumptions.

Because of the high pathloss, a large frequency offset would be required to preserve the gap between uplink and downlink signals at BS if FDD were assumed. Instead, TDD is considered.

The maximum transmit power of 20 dBm at the UE and 30 dBm are taken from [2], [3]. These transmit powers are reasonable since current CMOS RF power amplifiers in the mmW range exhibit peak efficiencies of at least 8%. This implies that the UE TX power of 20 dBm and BS TX power of 30 dBm can be achieved with powers of 1.25W and 12.5W, respectively.

B. Spatial patterning and beamforming

As described in the Introduction, an essential component of mmW systems is the ability to utilize very high-dimensional antenna arrays at the base station and mobile. In this work, we make the simplifying assumption that only single stream processing is considered and that beamforming is designed to maximize SNR without regard to interference. It is possible that more advanced techniques such as inter-cell coordinated beamforming and MIMO spatial multiplexing [15], [28], [29] may offer further gains, particularly for mobiles close to the cell. Thus, the gains of mmW systems may be even higher, although as we will see below, under our NLOS propagation models, many mobiles are power-limited and the gains of spatial multiplexing may be limited.

For the MIMO multipath channel model used in this paper, if perfect channel state information (CSI) is available at TX and RX, then the optimal instantaneous beamforming gain can be realized by transmitting and receiving along the singular directions. However, obtaining channel information is especially challenging in the mmW system due to large number of parameters used in the model. Therefore, to provide a feasible strategy as well as conservative performance estimates, the TX and RX perform long-term beaforming which aims at maximizing the average received power over many fading realizations and is based only on channel statistics. The detailed discussion is relegated to full paper [17].

C. SNR to Rate Mapping

In an actual cellular system, the achieved rate (goodput) will depend on the average SNR through a number of factors including the channel code performance, channel quality indicator (CQI) reporting, rate adaptation and Hybrid automatic repeat request (HARQ) protocol. In this work, we abstract this process and assume a simplified, but widely-used, model [30], where the spectral efficiency is assumed to be given by the Shannon capacity with some loss Δ:

$$\rho = \eta \min\left\{\log_2\left(1 + 10^{0.1(\mathsf{SNR}-\Delta)}\right), \rho_{max}\right\}, \qquad (2)$$

where ρ is the spectral efficiency in bps/Hz, the SNR and loss factor Δ are in dB, ρ_{max} is the maximum spectral efficiency and η is a bandwidth overhead factor to account for pilots, control messages and other signaling overhead. Calibrating the model (2) to a practical LTE system, the paper [30] suggests parameters $\Delta = 1.6$ dB and $\rho_{max} = 4.8$ bps/Hz. Assuming similar codes can be used for mmW system, we apply the same ρ_{max} in this simulation, but increase Δ to 3 dB to account for fading. The bandwidth overhead may be different in the mmW range since the control channels and pilot density may need to

change significantly. We assume a bandwidth efficiency factor of $\eta = 1$ for all calculations, except where we explicitly consider the overhead and set $\eta = 0.8$ as justified in [17]. Note that the rates computed in this paper *do not* include any half duplex loss. The rates after duplexing will depend on the duty cycle of TDD.

D. Downlink Scheduling

We use proportional fair scheduling with full buffer traffic. Since we assume that we cannot exploit multi-user diversity and only schedule on the average channel conditions, the proportional fair assumption implies that each UE will get an equal fraction of the time-frequency resources.

E. Uplink Scheduling

In uplink, we also assume full buffer traffic with proportional fair scheduling. In contract with the downlink, in the uplink different multiple access schemes result in different capacities. If BS allows one UE to transmit for a portion of time in the whole band, the total transmit power will be limited to the transmit power of one user. If all UEs are allowed to transmit all time but on different subbands, then the total transmit power will be multiplied by the number of UEs in the environment, which is advantageous for power limited systems. Therefore, we assume FDMA is performed in uplink unless otherwise stated. As discussed in the full paper [17], we observed negligible interference due to highly directional antennas, and hence power control was not necessary.

IV. Results and Discussion

A. Uplink and Downlink Capacity

We plot SINR and rate geometries in Fig. 2 and Fig. 3 respectively. The downlink and uplink have similar performance even though downlink TX power is 10 dB higher than the uplink. This is due to the fact that the uplink uses FDMA, where 10 UEs transmit simultaneously amounting to a 10-fold increase in total transmit power. It is also observed that for powers over 30 dBm for the downlink and 20 dBm for the uplink, the marginal improvement due to the increase of TX power starts to decline. Hence, in the rest of this paper, 30 dBm for downlink and 20 dBm for uplink are assumed unless otherwise stated.

Table III provides a comparison on mmW and current LTE systems based on capacity numbers in [13]. Compared to LTE, the mmW system provides a staggering 30-fold increase of overall cell capacity and more than 10-fold increase of cell edge rate. Operating bandwidth of mmW is chosen as 1 GHz different tha LTE. Nonetheless, this is reasonable when the overall potential bandwidth of mmW is considered. Given that this is only a bare-bone mmW system, we expect even higher gain when advanced technologies are applied to optimize the mmW system.

However, the 5% cell edge rates are less dramatic and only offer a 5 fold increase. This indicates a significant limitation of mmW systems under NLOS propagation edge of cell users become power-limited and are unable to exploit the increased spectrum. Thus, other features will be needed achieve a more uniform performance in mmW systems in these scenarios.

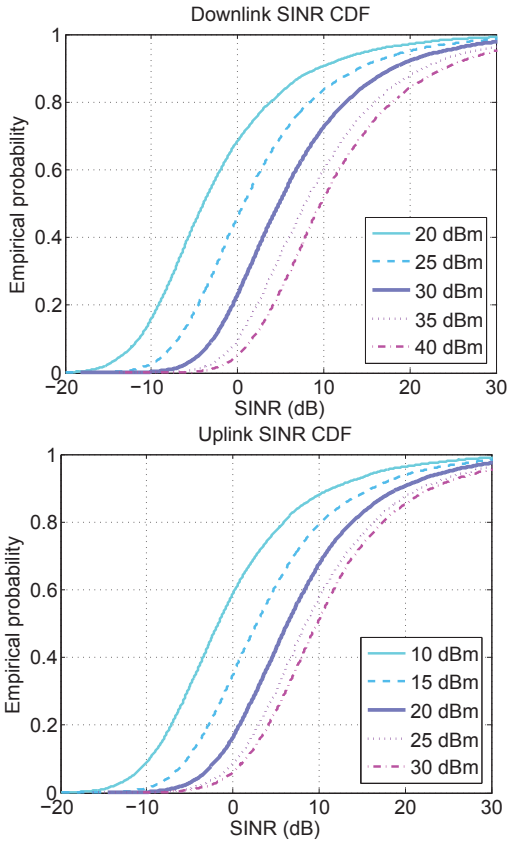

Fig. 2: Downlink (top plot) / uplink (bottom plot) SINR geometry with varying TX power

TABLE III: mmW and LTE cell capacity/cell edge rate comparison, assuming 20% overhead and 50% UL-DL duty cycle for mmW system

System antenna	BW & Duplex	fc (GHz)	Cell capacity (Mbps)	Cell edge rate (Mbps, 5%)
mmW 64x64	1 GHz TDD	28	780(DL) 850(UL)	97(DL) 128(UL)
LTE 2x2 DL, 2x4 UL	10+10 MHz FDD	2.5	26.9(DL) 23.6(UL)	9.0(DL) 9.7(UL)

B. Interference vs. Power-Limited Regime

The empirical cumulative distribution functions (CDF) of the downlink/uplink rate per UE are shown in Fig. 4. It is observed that although rate geometry generally improves as bandwidth increases, the marginal gain diminishes as bandwidth approaches 1 GHz. This implies that a mmW system with multi-GHz bandwidth is power-limited and the degrees of freedom in the bandwidth are likely to be under-utilized. As a result, multiple antennas should be operated in the beamforming mode to reduce signal attenuation due to path loss, rather than the spatial multiplexing mode, which benefits

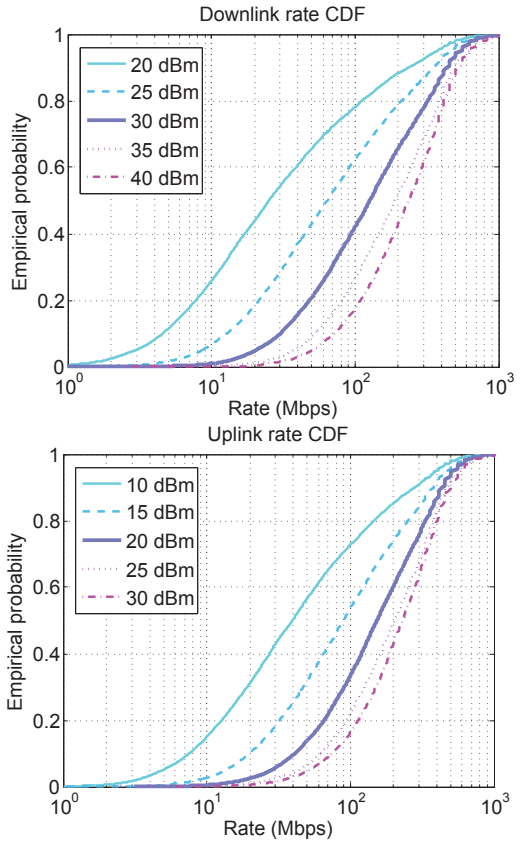

Fig. 3: Downlink (top plot) / uplink (bottom plot) rate geometry with varying TX power

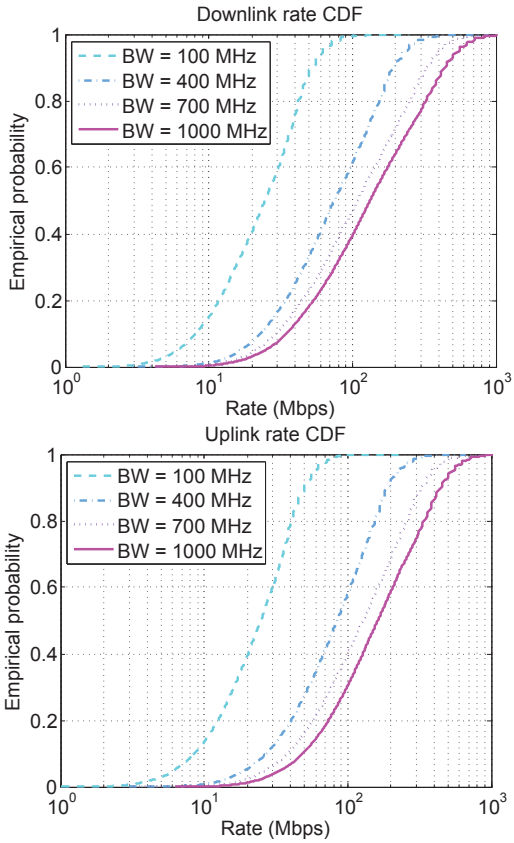

Fig. 4: Downlink (top plot) / uplink (bottom plot) rate geometry with varying bandwidth

only in the high power regime.

The cell effective SINR is shown in Fig. 5 with varying TX power. It is clear that the effective SINR changes linearly with respect to TX power, again indicating that mmW system is power-limited rather than interference-limited. Consequently, interference management technologies such as power control, coordinated beamforming, and interference cancellation will have less impact on mmW system than they do in the LTE system. On the other hand, multihop relaying, as a method of reducing TX-RX distance, may play a much more important role in mmW, since the bottleneck is no longer the degrees of freedom, but rather the raw received power, a scenario that is the exact opposite of the current interference-limited cellular system.

C. Implications for Device Requirements and Multiple Access

As pointed out in prior work [2], [3], the cost of implementing analog-to-digital converter (ADC) and digital-to-analog converter (DAC) that are capable of supporting multi-Gbps transmission could be prohibitive for a mmW system with large antenna arrays. Hence, it may be favorable to choose RF beamforming (one ADC/DAC per RF chain, beamform to one direction at a time) over digital beamforming (one ADC/DAC per antenna, beamform to multiple directions simultaneously) by forgoing the support of multi-stream and multi-user transmissions. However, according to the uplink rate geometry

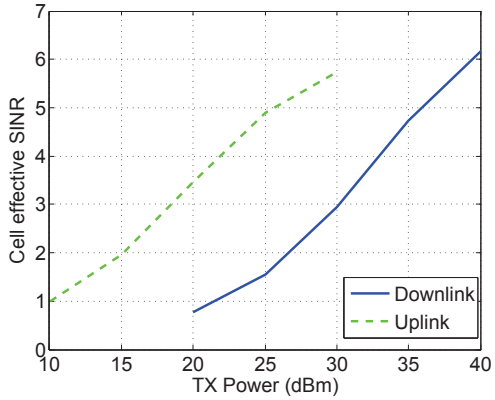

Fig. 5: Downlink/uplink effective SINR computed from cell average spectral efficiency

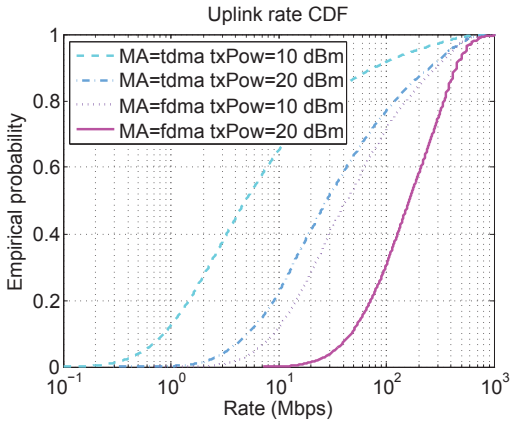

Fig. 6: Uplink rate geometry vs multi-access schemes

shown in Fig. 6, one can easily see an order of magnitude improvement when multi-user transmission is enabled by FDMA, compared to a baseline TDMA. Despite the high cost, there is still very good motivation to pursue multi-user support and advance technologies aiming at reducing complexity/cost of ADC/DAC [31] that will likely to play a vital role in a practical multi-Gbps mmW system deployment.

V. Conclusions

In this paper we have provided system level simulations to evaluate the capacity of mmW cellular systems using channel models based on urban experimental path loss data. Our results have shown that mmWave systems can provide 30-fold improvement in data rates compared with the current LTE systems. However, because of the dominance of the NLOS paths, the mmWave system becomes power limited rather than interference limited, necessitating different design methodologies than the current LTE systems. Future research directions include power efficient beamforming at different subbands in order to utilize FDMA in uplink and multihop relaying in downlink to exploit the unused degrees of freedom and to extend the range.

References

[1] Cisco, "Cisco Visual Network Index: Global mobile traffic forecast update," 2012.

[2] F. Khan and Z. Pi, "Millimeter-wave Mobile Broadband (MMB): Unleashing 3-300GHz Spectrum," in *Proc. IEEE Sarnoff Symposium*, Mar. 2011.

[3] ——, "An introduction to millimeter-wave mobile broadband systems," *IEEE Comm. Mag.*, vol. 49, no. 6, pp. 101 – 107, Jun. 2011.

[4] T. Rappaport, J. Murdock, and F. Gutierrez, "State of the art in 60-GHz integrated circuits and systems for wireless communications," *Proceedings of the IEEE*, vol. 99, no. 8, pp. 1390 – 1436, August 2011.

[5] C. Doan, S. Emami, D. Sobel, A. Niknejad, and R. Brodersen, "Design considerations for 60 GHz CMOS radios," *IEEE Comm. Mag.*, vol. 42, no. 12, pp. 132 – 140, 2004.

[6] E. Perahia, C. Cordeiro, M. Park, and L. Yang, "IEEE 802.11ad: Defining the next generation multi-Gbps Wi-Fi," in *Proc. IEEE Cons. Comm. & Network. Conf.*, Jan. 2010.

[7] S. J. Vaughan-Nichols, "Gigabit Wi-Fi is on its way," *IEEE Computer*, Nov. 2010.

[8] T. Baykas, C.-S. Sum, Z. Lan, J. Wang, M. A. Rahman, H. Harada, and S. Kato, "IEEE 802.15.3c: The first IEEE wireless standard for data rates over 1 Gb/s," *IEEE Comm. Mag.*, Jul. 2011.

[9] Y. Azar, G. N. Wong, K. Wang, R. Mayzus, J. K. Schulz, H. Zhao, F. Gutierrez, D. Hwang, and T. S. Rappaport, "28 GHz propagation measurements for outdoor cellular communications using steerable beam antennas in New York City," in *Proc. ICC (to appear)*, 2013.

[10] H. Zhao, R. Mayzus, S. Sun, M. Samimi, J. K. Schulz, Y. Azar, K. Wang, G. N. Wong, F. Gutierrez, and T. S. Rappaport, "28 GHz millimeter wave cellular communication measurements for reflection and penetration loss in and around buildings in New York City," in *Proc. ICC (to appear)*, 2013.

[11] M. Samimi, K. Wang, Y. Azar, G. N. Wong, R. Mayzus, H. Zhao, J. K. Schulz, S. Sun, F. Gutierrez, and T. S. Rappaport, "28 GHz angle of arrival and angle of departure analysis for outdoor cellular communications using steerable beam antennas in New York City," in *Proc. IEEE VTC (to appear)*, 2013.

[12] ——, "28 GHz path loss models in New York City," in *Proc. Globecomm (submitted)*, 2013.

[13] 3GPP, "Further advancements for E-UTRA physical layer aspects," TR 36.814 (release 9), 2010.

[14] ITU, "M.2134: Requirements related to technical performance for IMT-Advanced radio interfaces," Technical Report, 2009.

[15] H. Zhang, S. Venkateswaran, and U. Madhow, "Channel modeling and MIMO capacity for outdoor millimeter wave links," in *Wireless Communications and Networking Conference (WCNC)*, April 2010.

[16] S. Akoum, O. E. Ayach, and R. W. Heath, "Coverage and capacity in mmWave MIMO systems," in *Proc. of Asilomar Conf. on Signals, Syst. & Computers*, Pacific Grove, CA, Nov. 2012.

[17] M. R. Akdeniz, Y. Liu, S. Rangan, and E. Erkip, "Millimeter wave picocellular system evaluation for urban deployments," arXiv preprint, Mar. 2013.

[18] T. Zwick, T. Beukema, and H. Nam, "Wideband channel sounder with measurements and model for the 60 GHz indoor radio channel," *IEEE Trans. Vehicular Technology*, vol. 54, no. 4, pp. 1266 – 1277, July 2005.

[19] F. Giannetti, M. Luise, and R. Reggiannini, "Mobile and personal communications in 60 GHz band: A survey," *Wirelesss Personal Comunications*, vol. 10, pp. 207 – 243, 1999.

[20] C. Anderson and T. Rappaport, "In-building wideband partition loss measurements at 2.5 and 60 GHz," *IEEE Wireless Comm.*, vol. 3, no. 3, pp. 922 – 928, May 2004.

[21] P. Smulders and A. Wagemans, "Wideband indoor radio propagation measurements at 58 GHz," *Electronics Letters*, vol. 28, no. 13, pp. 1270 –1272, June 1992.

[22] T. Manabe, Y. Miura, and T. Ihara, "Effects of antenna directivity and polarization on indoor multipath propagation characteristics at 60 GHz," *IEEE J. Sel. Areas Comm.*, vol. 14, no. 3, pp. 441 –448, April 1996.

[23] H. Xu, V. Kukshya, and T. Rappaport, "Spatial and temporal characteristics of 60 GHz indoor channel," *IEEE J. Sel. Areas Comm.*, vol. 20, no. 3, pp. 620 – 630, April 2002.

[24] E. Torkildson, H. Zhang, and U. Madhow, "Channel modeling for millimeter wave MIMO," in *Proc. Information Theory and Applications Workshop (ITA)*, Feb. 5 2010.

[25] H. Zhang and U. Madhow, "Statistical modeling of fading and diversity for outdoor 60 GHz channels," in *International Workshop on mmWave Communications: from Circuits to Networks (mmCom10)*, September 2010.

[26] E. Ben-Dor, T. Rappaport, Y. Qiao, and S. Lauffenburger, "Millimeter-wave 60 GHz Outdoor and Vehicle AOA Propagation Measurements using Broadband Channel Sounder," in *Proc. IEEE Globecom*, Dec. 2011.

[27] T. S. Rappaport, *Wireless Communications: Principles and Practice*, 2nd ed. Upper Saddle River, NJ: Prentice Hall, 2002.

[28] A. Alkhateeb, O. E. Ayach, G. Leus, and J. Robert W. Heath, "Hybrid analog-digital beamforming design for millimeter wave cellular systems with partial channel knowledge," in *Proc. Information Theory and Applications Workshop (ITA)*, Feb. 2013.

[29] O. Ayach, R. Heath, S. Abu-Surra, S. Rajagopal, and Z. Pi, "Low complexity precoding for large millimeter wave MIMO systems," in *Proc. ICC*, June, pp. 3724–3729.

[30] P. Mogensen, W. Na, I. Z. Kovács, F. Frederiksen, A. Pokhariyal, K. I. Pedersen, T. Kolding, K. Hugl, and M. Kuusela, "LTE capacity compared to the Shannon bound," in *Proc. IEEE VTC*, 2007.

[31] H. Zhang, S. Venkateswaran, and U. Madhow, "Analog multitone with interference suppression: Relieving the ADC bottleneck for wideband 60 ghz systems," in *Proc. Globecomm*, Nov. 2012.